GEOPHYSICS, VOL. 55, NO. 5 (MAY 1990); P. 521–526, 8 FIGS.

Finite-difference calculation of traveltimes in three dimensions

John E. Vidale*

ABSTRACT

The traveltimes of first arriving seismic rays through most velocity structures can be computed rapidly on a three-dimensional numerical grid by finite-difference extrapolation. Head waves are properly treated and shadow zones are filled by the appropriate diffractions. Differences of less than 0.11 percent are found between the results of this technique and ray tracing for a complex but smooth model. This scheme has proven useful for earthquake location and shows promise as an inexpensive, well-behaved substitute for ray tracing in forward-modeling and Kirchhoff inversion applications.

INTRODUCTION

Transit times for seismic waves are computed in a variety of ways. Herein, I describe the extension to three dimensions of the two-dimensional (2-D) finite-difference method of Vidale (1988). Currently, there are two classes of solutions to the problem of ray tracing seismic velocity structures, each with different types of difficulties. The simpler schemes for computing traveltimes assume a one-dimensional (1-D) velocity structure, which allows simple and inexpensive results. These methods produce errors to the extent that the velocity structure deviates from being solely depth-dependent, both from incorrect raypaths and from integration of incorrect slownesses along the raypath. The less simple schemes trace rays through 2-D or three-dimensional (3-D) velocity structures (Červeny et al., 1977; Julian and Gubbins, 1977). Ray tracing can produce the correct answer but is computationally intensive, frequently encounters shadow zones, and sometimes picks the wrong raypath as the first arrival.

Approximations can alleviate these difficulties: Thurber (1981) reduces the 3-D problem to two dimensions for economy; Thurber (1983) smooths the structures until ray tracings are well-behaved; Roecker (1982) finds the raypath with 1-D structure but integrates in a 3-D slowness field to find the traveltime; and Um and Thurber (1987) and Prothero et al. (1988) use perturbation methods in three dimensions.

This paper presents a finite-difference method that computes the first-arrival time with no approximations and few potential problems. We are already using this scheme for earthquake location (Nelson and Vidale, 1990) and forward modeling to determine velocity structure. The procedure is similar to but more general than the 2-D finite-difference method proposed by Reshef and Koslof [1986, equation (5)] and differs from the finite-element scheme of Virieux et al. (1988) in that isochrons rather than geometric rays are used.

METHOD

The method is formulated for a velocity structure that is sampled at discrete points in a 3-D space, with equal horizontal and vertical spacing. The question of what continuous structure is implied by the sampled structure is more complicated; for testing purposes, I compare the results with analytic solutions for a uniform medium and with a ray-tracing scheme in which the velocity structure is interpolated linearly between the sampled points. An array of the same dimension as the velocity structure is created to record the traveltimes. These two arrays use the bulk of the computer memory in this method.

The calculation begins with the identification of the grid point nearest the source location (the source need not coincide with a grid point). The traveltime to each grid point in the 5 by 5 by 5 point volume surrounding the nearest grid point is calculated by integrating the slowness from the origin to the point, assuming a straight raypath. (The calculation could begin with the 3 by 3 by 3 point volume, but errors from the curvature of the wavefront are greater than the errors from the assumption of a straight raypath.) The next step is to calculate the traveltimes to the 7 by 7 by 7 box containing the 5 by 5 by 5 volume with the method outlined below. This step is followed by the calculation of the 9 by 9 by 9 box containing the 7 by 7 by 7 box, and so on until the

Manuscript received by the Editor April 7, 1989; revised manuscript received August 23, 1989.
*C. F. Richter Seismological Laboratory, Earth Sciences, University of California, Santa Cruz, Santa Cruz, CA 95064.

six faces of the box have encountered the six sides of the rectangular prism on which the wave slowness is specified. This iterative process is directly analogous to the solution for rings of increasing radius in the 2-D method of Vidale (1988).

In the description of the method, I first show the method to extrapolate traveltimes from point to point, then show the order in which the grid points are solved. The iterative extrapolation is based on the eikonal equation of ray tracing

$$\left(\frac{\partial t}{\partial x}\right)^2 + \left(\frac{\partial t}{\partial y}\right)^2 + \left(\frac{\partial t}{\partial z}\right)^2 = s^2(x, y, z) \qquad (1)$$

that relates the gradient of the traveltime to the velocity structure (see, for example, Officer, 1974, p. 203). t is the traveltime, the Cartesian coordinate axes are x, y, and z, and s is the slowness (inverse of velocity).

The method to compute traveltimes in this paper uses three different schemes based on equation (1) for three different situations described below. The geometries of the grid points involved in each of the three methods are shown in Figure 1. Scheme A, which is typically used more than 90 percent of the time is shown in Figure 1a. Once the traveltimes for seven of the corners of a cube are known, the eighth may be found by applying finite differencing to equation (1) to obtain

$$t_7 = t_0 + \frac{1}{\sqrt{2}}\sqrt{6h^2s^2 - (t_1 - t_2)^2 - (t_2 - t_4)^2 - (t_4 - t_1)^2 - (t_3 - t_5)^2 - (t_5 - t_6)^2 - (t_6 - t_3)^2}, \qquad (2)$$

where h is the mesh spacing and t_i is the traveltime to the ith point. The slowness s used is the average of the slownesses at the eight corners of the cube. This formula was derived by Richard Stead (California Institute of Technology, 1988, Pers. comm.). The accuracy of this centered finite-difference formula for a uniform velocity case is shown in Figures 2 and 3.

When the source is placed at a distance of ten times the grid spacing from the point 0 in Figure 1a (whose time is t_0) in a uniform velocity structure, the error in the extrapolation of traveltime to point 7 reaches a maximum of 1 percent of the difference between traveltimes at points 0 and 7. Figure 3 shows that the error diminishes rapidly with increasing distance or equivalently decreasing curvature of the isochrons. This formula produces the correct traveltime for any plane wave and for spherical waves traveling along the diagonal from point 0 to point 7.

Scheme B, which is shown in Figure 1b, is used to compute more than 90 percent of the traveltimes that are not computed with method A. The traveltime to point 5 is extrapolated from points 0 through 4 by the formula

$$t_5 = t_1 + \sqrt{2h^2s^2 - 0.5(t_0 - t_3)^2 - (t_2 - t_4)^2}. \qquad (3)$$

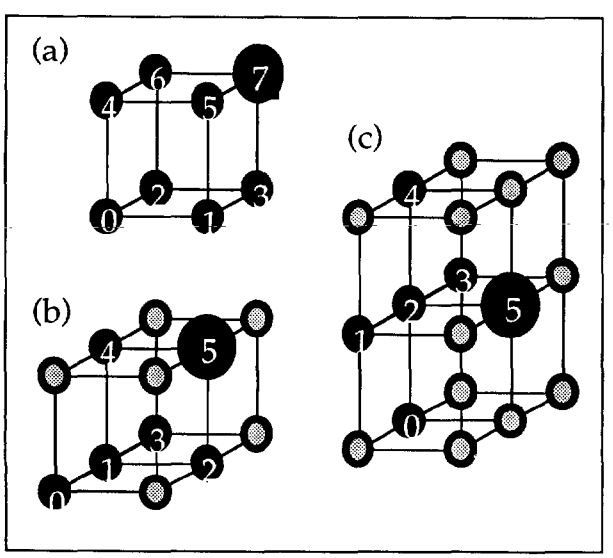

FIG. 1. The geometry of the three basic stencils used as the building blocks for computing the traveltimes on a uniformly spaced 3-D grid. (a) The traveltimes to points 0 through 6 are used to compute the traveltime to point 7 with equation (2). (b) Points 0 through 4 used to compute point 5 with equation (3). (c) Points 0 through 4 used to compute point 5 with equation (4). Light circles indicate points that are not used.

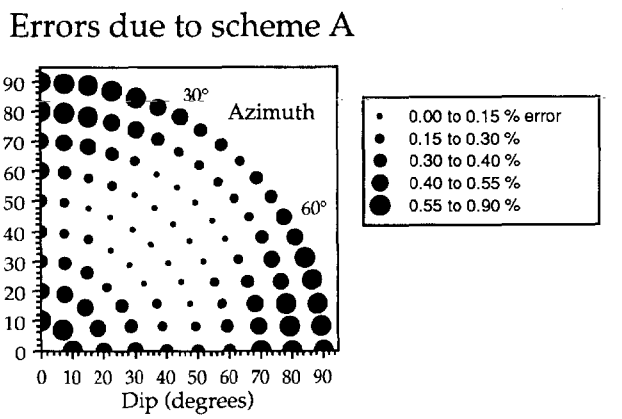

FIG. 2. The error arising from the solution of equation (2) for a uniform medium at a range of 10 grid points. The error is plotted as a function of the dip and the strike of the vector connecting the source point and point 7 in Figure 1a, so the plot covers a quarter of a hemisphere. The symmetry reflecting the equivalence of the x-axis (strike of 90°, dip of 90°), y-axis (strike of 0°, dip of 90°), and z-axis (dip of 0°) is easily seen.

The slowness s in equation (3) is the average of the slownesses to the centers of the two cubes shown in Figure 1b (which are each the average of the slowness to the eight corners of its cube). Scheme B does not use centered finite differences. A centered scheme can be made by selecting points 1, 2, and 4 to be twice as far from point 5 as is shown in Figure 1b; but compactness is chosen over improved accuracy, and a quick check showed little difference between the two options. The accuracy of method B for a uniform velocity case is shown in Figure 4.

Scheme C, shown in Figure 1c, is used for the calculation of the fewest traveltimes. The traveltime to point 5 is extrapolated from points 0 through 4 by the formula

$$t_5 = t_2 + \sqrt{h^2 s^2 - 0.25[(t_1 - t_3)^2 + (t_0 - t_4)^2]}. \quad (4)$$

Here I have used the average of the slownesses in each of the four cubes shown in Figure 1c for slowness s (each slowness is the average of the slownesses at the eight corners of its cube). The accuracy of method C for a uniform velocity case is shown in Figure 5. In equations (2), (3), and (4) most of the computational expense is due to the one square root. Scheme C also does not use centered finite differences, again because a centered scheme would be less compact. Equations (3) and (4) are the 3-D equivalents of the 2-D case [Vidale, 1988, equation (6)].

The solution stems from the ability to calculate the traveltimes iteratively at any point on a cube from equation (2), (3), or (4), whether the point is on a face, a side, or a corner of the rectangular prism. The key step I have not yet described is how the traveltimes in each shell (at each radius) are determined. The simplest schemes that are independent of the relative timing of the grid points fail because the finite-difference operators sometimes lie across the cusps in traveltime. This situation results from the discontinuous changes in the first-arrival raypath where there are triplications or bow-tie patterns of multiple arrivals.

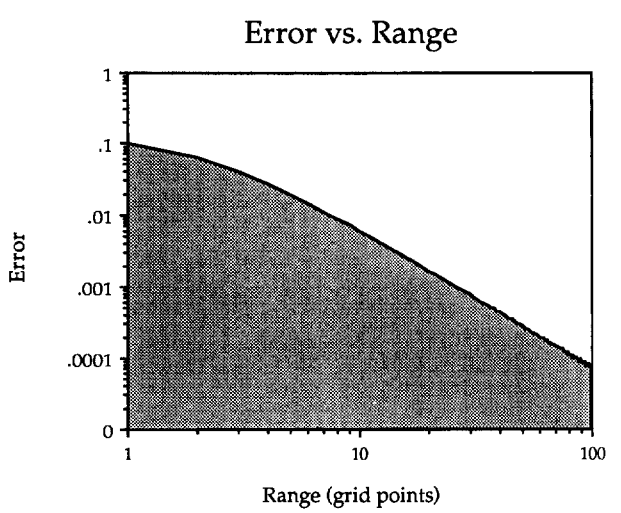

FIG. 3. The falloff of the error with increasing range (decreasing curvature) in a uniform medium. One of the directions from Figure 2 (strike of 90°, dip of 90°) with maximum error is chosen. The error falls to about 1 percent by a distance of ten grid points, as also shown in Figure 2.

When no side of the shell has encountered a side of the computational grid, the shell has six sides, twelve edges, and eight corners. Each is dealt with separately. Figure 6 shows such a side. Ignoring the points constituting the perimeter of the side, there are nine (3 by 3) grid points per side whose traveltimes are to be calculated. The nine traveltimes for the points just behind the side are known from calculating the traveltimes on the previous box, and they are used in the

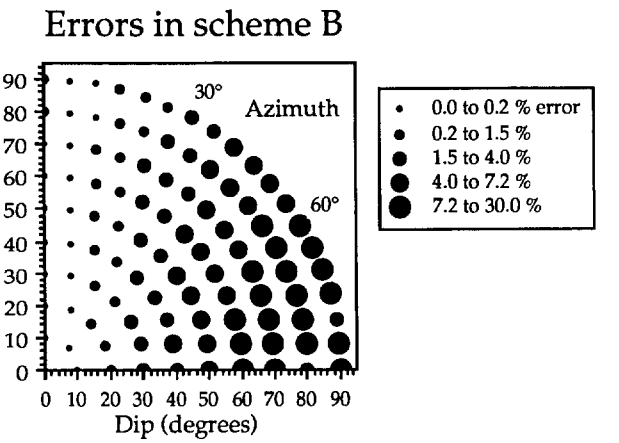

FIG. 4. The error arising from the solution of equation (3) for a uniform medium at a range of 10 grid points. The error is plotted as a function of the dip and the strike of the vector connecting the source point and point 5 in Figure 1b, and the plot covers a quarter of a hemisphere. This equation applies to two quarter-hemispheres, only one of which is shown. Reflection across a plane at an azimuth of 0° shows the full range of application. The solution is most accurate near this azimuth of 0°, which is, not coincidentally, the principal direction that the seismic energy is traveling when this equation is invoked.

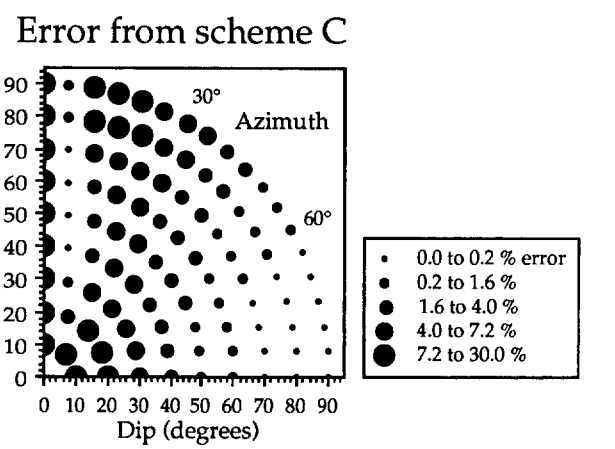

FIG. 5. The error arising from the solution of equation (4) for a uniform medium at a range of 10 grid points. The error is plotted as a function of the dip and the strike of the vector connecting the source point and point 5 in Figure 1c, and the plot covers a quarter of a hemisphere. This equation is applied to an entire hemisphere that may be seen by reflecting across the two planes at (1) an azimuth of 90° and (2) a dip of 90°. The solution is most accurate near the azimuth of 90° and the dip of 90°, which is the direction the seismic energy is traveling when this equation is invoked.

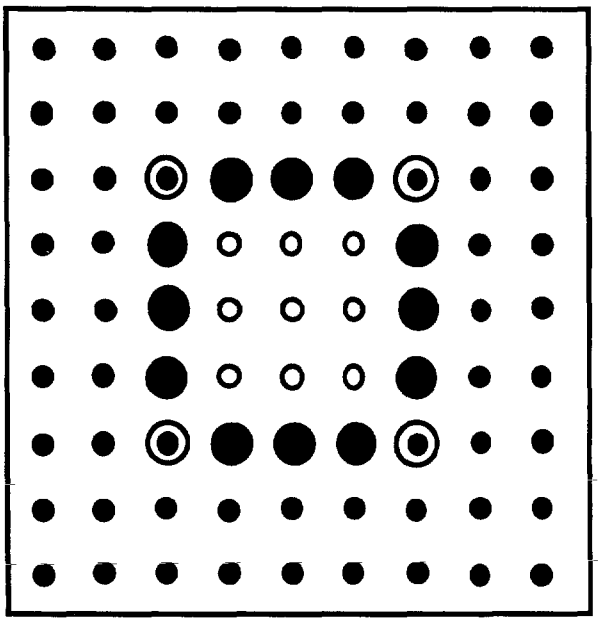

FIG. 6. The solution for the traveltime to each point in the grid is broken down to the solution for a sequence of cubes of increasing radius from the grid point closest to the source. This figure illustrates one of the six sides of one cube. The small, black dots are outside the cube. The text describes how the traveltimes from the source to the points marked by hollow circles are first solved on this and the five other sides. Second, the traveltimes to the simple, large black dots on the four edges shown and the eight edges not shown are calculated. Third, the traveltimes to the four corners marked by double circles as well as the four corners not shown are found. Next, the cube of points just outside the cube pictured is considered, and its sides, edges, and corners are timed, and so on.

solution for the times of the points on this side of the current box.

The solution for the traveltimes proceeds as follows: all the points on the side to be timed (the hollow circles in Figure 6) are sorted in order of increasing traveltime for the point just behind them in the previous box. I then consider each point in order of increasing traveltime. A point that is at a relative minimum in traveltime has none of its four closest neighbors on the current box timed, so scheme C is used to extrapolate its traveltime from the five traveltimes at points just behind it on the previous box. Since, by my choice of point 2, the traveltime to point 2 in Figure 1c is less than the traveltime to points 0, 1, 3, and 4, the seismic raypath is nearly normal to the side (azimuth of 90° and dip of 90°) and is in the region of high accuracy in Figure 5.

At a point that has just one of its four closest neighbors timed, scheme B estimates the traveltime from the one neighbor on the current side and four other neighbors on the previous side. This situation arises at the points nearest to the point determined by scheme C in the previous paragraph (among others). Since the traveltime to point 1 in Figure 1b is less than the times to points 0 and 3, the seismic raypath lies nearly in the plane containing points 1, 2, 4, and 5. This direction (with strike near 0°) has good accuracy, as is shown in Figure 4.

If two adjacent nearest neighbors as well as the diagonal neighbor between them on the current side are timed, the most accurate extrapolation, scheme A, is used. Most points are timed by scheme A. Occasionally, two arrivals approach the point nearly simultaneously. The correct answer is obtained by estimating arrival times for both paths and adopting the earlier of the two.

By applying this algorithm to every grid point on the side in order of increasing traveltime, the traveltimes for the entire side are determined. It does not matter in which order the six sides are solved.

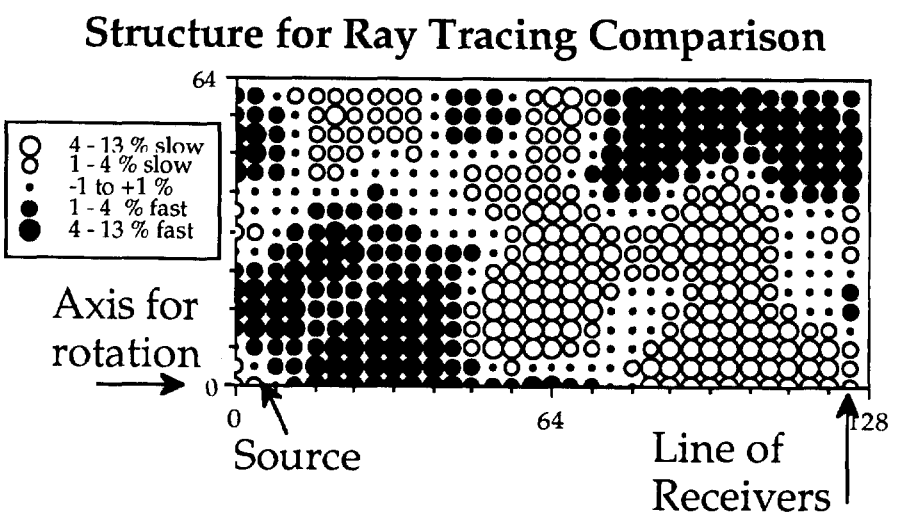

FIG. 7. The velocity model used to compare the finite-difference traveltimes with the ray-tracing traveltimes. Filled circles represent fast velocity, hollow circles show slow velocity, and larger circles indicate more anomalous velocities. The rms velocity variation is 5 percent and the grid has 64 by 128 points, although it is resampled for this figure. The correlation length is 20 grid points.

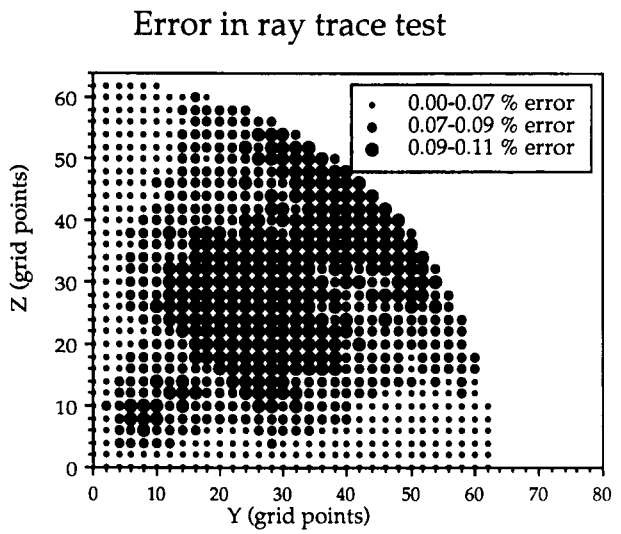

FIG. 8. Comparison of finite-difference with ray-tracing traveltimes for the structure shown in Figure 7. The discrepancy between the traveltime computed for the top layer of grid points with the 3-D finite-difference algorithm and the 2-D ray tracer is plotted as a function of y and z, the grid coordinates. The point $(y, z) = (0, 0)$ lies directly to the right of the source point. The largest error is 0.11 percent, or about one-tenth of a second for a traveltime of 100 s.

The edges are simpler. Consider the left edge in Figure 6, which has three grid points. Remember that the traveltimes to the sides of the current box have already been determined. As with the ordering of the sides, the points on the edge are ordered with respect to increasing traveltime on the edge of the previous box. The traveltimes are calculated in order. Each grid point on the current edge has two neighbors that are also on the current edge. If neither neighbor has yet been computed, the traveltime is extrapolated from two neighbors on the current sides and three points from the previous edge by scheme B. If one neighbor has already been calculated, that neighbor, four points on the current sides, and two points from the previous edge are used in the extrapolation with scheme A. If both neighbors have been computed, each is used with equation (2) to estimate a traveltime and the earlier of the two is adopted as the true traveltime. The order of solution for the edges does not matter.

Each current corner has three points on the current sides, three points on the current edges, and one point on the previous corner that are already timed in the geometry of Figure 1a. Scheme A is then used to compute the time to the corner from these seven known traveltimes.

COMPARISON OF FINITE DIFFERENCES WITH RAY TRACING

Although uniform media are useful for checking the accuracy of computational techniques, computing accurate traveltimes for uniform media is not of great practical use. The finite-difference traveltime algorithm may be tested against a 2-D ray-tracing technique as follows: The 2-D random medium shown in Figure 7 is constructed with an rms velocity variation of 5 percent.

The traveltimes through this structure have been computed by ray tracing with the method of Stork (1988) in Vidale's (1988) paper. A 3-D velocity structure with cylindrical symmetry is constructed by spinning the 2-D structure in Figure 7 around its lower edge. Since the source is on the axis of the cylindrical symmetry, the raypaths through the structure remain in the plane containing the axis and the receiver. The traveltimes computed with the finite-difference algorithm through the 3-D structure may be compared with those from the ray tracer. This procedure tests the ability of the finite-difference algorithm to track wavefronts accurately in many directions.

The finite-difference and the ray-tracing traveltimes agree to within 0.11 percent for all grid points on the right surface, as shown in Figure 8. The variations in traveltime for this model compared to a model with a uniform velocity structure range up to 5 percent. This model is complex enough to cause difficulties for the ray tracer such as losing rays (shadow zones) and picking a secondary arrival as the first arrival (multipathing combined with a shadow zone). Although it is not clear from this test, the finite-difference scheme is formulated to treat head waves and diffractions properly, and we have tested this claim in several earthquake location applications (Nelson and Vidale, 1990).

Rules of thumb for usage are few. The attempt to follow a ray which flows in a direction counter to the order of solution leads to trouble. More explicitly, if a velocity contrast is more than a factor of two, a raypath, if correctly determined, might well progress from the region outside one of the boxes back inside the box. Clearly, with the method outlined, this ray is not timed accurately, since the area outside the box currently being solved has not yet been timed. This problem appears numerically as the square roots in equations (2) through (4) containing negative numbers. The most robust fix is to set the square roots to zero, which simulates rays traveling parallel to the boundary, but the answer in general is not correct.

The numbers quoted in this paper come from propagating about 100 grid points; better performance can be expected from finer grids, worse from coarser grids. A finer grid leads to more accurate traveltimes. In the case of velocity variations that are smooth enough that the errors shown in Figures 2 and 3 are negligible far from the source, doubling the number of grid points traversed halves the error.

The traveltime fields of numbers can be converted to amplitudes by consideration of takeoff angles and geometrical spreading (see Vidale and Houston, 1990).

CONCLUSIONS

Traveltimes may be computed accurately through arbitrary 3-D velocity fields by finite-difference techniques. Comparisons with a ray-tracing method show that traveltimes computed across grids with dimensions of the order of 100 by 100 by 100 grid points have errors of less than 0.11 percent for smooth models. This technique, which is useful for a variety of applications, including iterative velocity inversion and Kirchhoff migration methods, promises to make computation of large numbers of traveltimes routine.

ACKNOWLEDGMENTS

Support for this work has been provided in part by Institute of Geophysics and Planetary Physics grant 88-37, a grant from the W. M. Keck Foundation, and the Institute of Tectonics, University of California, Santa Cruz. Reviews by Quentin Williams and Heidi Houston helped the text. Richard Stead, Christof Stork, and Robert Clayton contributed ideas. Contribution no. 68 from the Charles F. Richter Seismological Laboratory at the University of California, Santa Cruz.

REFERENCES

Červeny, V., Molotkov, I. A., and Pšenčik, I., 1977, Ray methods in seismology: Univ. of Karlova Press.

Julian, B. R., and Gubbins, D., 1977, Three-dimensional seismic ray tracing: J. Geophys. Res., **43**, 95–114.

Nelson, G. D., and Vidale, J. E., 1990, Earthquake location with finite-difference traveltimes in Bear Valley, Ca.: Bull., Seis. Soc. Am., in press.

Officer, C. B., 1974, Introduction to theoretical geophysics: Springer-Verlag.

Prothero, W. A., Taylor, W. J., and Eickemeyer, J. A., 1988, A fast, two-point, three-dimensional raytracing algorithm using a simple step search method: Bull., Seis. Soc. Am., **78**, 1190–1198.

Reshef, M., and Kosloff, D., 1986, Migration of common shot gathers: Geophysics, **51**, 324–332.

Roecker, S. W., 1982, Velocity structure of the Pamir-Hindu Kush region: possible evidence of subducted crust: J. Geophys. Res., **87**, 945–959.

Stork, C., 1988, Ray trace tomographic velocity analysis of surface seismic reflection data: Ph.D. thesis, California Inst. of Tech..

Thurber, C. H., 1981, Earth structure and earthquake locations in the Coyote Lake area, central California: Ph.D. thesis, Massachusetts Inst. of Tech..

——— 1983, Earthquake locations and three-dimensional crustal structure in the Coyote Lake area, central California: J. Geophys. Res., **88**, 8226–8236.

Um, J., and Thurber, C. H., 1987, A fast algorithm for two-point seismic ray tracing: Bull., Seis. Soc. Am., **70**, 972–986.

Vidale, J. E., 1988, Finite-difference traveltime calculation: Bull., Seis. Soc. Am., **78**, 2062–2076.

Vidale, J. E., and Houston, H. B., 1990, Rapid calculation of seismic amplitudes: Geophysics, submitted.

Virieux, J., Ferra, V., and Madariaga, R., 1988, Ray tracing for earthquake location in laterally heterogeneous media: J. Geophys. Res., **93**, 6585–6600.